

Reconstructed properties of the sources of UHECR and their dependence on the extragalactic magnetic field

David Wittkowski^{*a} for the Pierre Auger Collaboration^b

^a*Department of Physics, Bergische Universität Wuppertal, Gaußstraße 20, D-42097 Wuppertal, Germany*

^b*Pierre Auger Observatory, Av. San Martín Norte 304, 5613 Malargüe, Argentina*

E-mail: auger_spokespersons@fnal.gov

Full author list: http://www.auger.org/archive/authors_icrc_2017.html

We present simulations of the propagation of ultra-high energy cosmic rays (UHECR) in three-dimensional space, including realistic assumptions about the extragalactic magnetic field (EGMF) and taking into account interactions of the UHECR with the cosmic microwave background and extragalactic background light as well as the cosmological evolution of the universe. On this basis, we study which energy spectrum and chemical composition of the UHECR must be assumed at their sources to obtain an energy spectrum and a chemical composition of the UHECR arriving at Earth that are in best agreement with the measurements by the Pierre Auger Observatory. We find that the best-fitting energy spectrum and chemical composition parameters depend strongly on the properties of the EGMF, showing that the EGMF must be carefully taken into account. Furthermore, we address the dependence of these parameters on the source evolution.

*35th International Cosmic Ray Conference – ICRC2017
10-20 July, 2017
Bexco, Busan, Korea*

^{*}Speaker.

1. Introduction

Two of the main unresolved questions in high energy astrophysics concern the origin of ultra-high-energy cosmic rays (UHECR, particles with energies ≥ 1 EeV) and the properties of their sources [1, 2]. To address these fundamental questions, the propagation of UHECR from their sources to Earth is simulated under assumptions regarding the sources as well as interaction effects in the propagation of UHECR through the universe. The energy spectrum and chemical composition of the simulated UHECR events arriving at Earth are then compared to those of actual UHECR measured at Earth. Recently, such a comparison has been made between simulation results based on a one-dimensional (1D) astrophysical model and measurements from the Pierre Auger Observatory [3]. By fitting the model to the experimental data, information on the energy spectrum and chemical composition of the UHECR at the sources have been obtained.

The most important assumptions that affect the simulation results concern the positions of the sources, the energy spectrum and chemical composition of the UHECR at the sources, the cosmic microwave background (CMB) and extragalactic background light (EBL) with which the UHECR can interact, and the extragalactic magnetic field (EGMF) that bends the trajectories of charged particles. While the CMB is known with high accuracy and the influence of the EBL on the simulation results was recently addressed alongside other influences in [3], the dependence of the simulation results on the other assumptions still needs to be studied in detail. Common simplifications in previous simulation studies are assuming a homogeneous distribution of the UHECR sources, although we can expect that the real sources are discrete objects that follow the mass distribution of the universe, and 1D simulations, which consider only one spatial degree of freedom and are therefore not able to take, e.g., the structured spatially anisotropic EGMF appropriately into account.

Going beyond these previous studies, here we investigate the propagation of UHECR by elaborate four-dimensional (4D) simulations, which take into account all three spatial degrees of freedom as well as the cosmological time-evolution of the universe, and consider discrete sources whose distribution follows the local mass distribution of the universe. On this basis we study for which energy spectrum and chemical composition at the sources the simulated energy spectrum and chemical composition at Earth are in the best possible agreement with the latest data from the Pierre Auger Observatory, and how this depends on the EGMF.

2. Methods

2.1 Simulation of the UHECR propagation

To simulate the propagation of UHECR from their sources to Earth, we used the 4D mode of the Monte Carlo code CRPropa 3 [4]. The sources were assumed to be discrete objects and their positions were chosen randomly following the large-scale structure of Dolag et al. [5], which is a common model for the local mass distribution of the universe. To avoid effects of near-Earth sources, which are influenced only marginally by the EGMF, we considered sources with a minimal distance $d_{\min} = 10$ Mpc from the observer. For the maximal redshift of the sources we chose $z \approx 1.3$, which is equivalent to a maximal comoving distance $d_{\max} \approx 4$ Gpc. Considering known bounds on the source density ρ [6], we chose $\rho \approx 10^{-4} \text{ Mpc}^{-3}$. Furthermore, we assumed that all sources are similar and that they isotropically emit particles consisting of the five representative elements ^1H ,

${}^4\text{He}$, ${}^{14}\text{N}$, ${}^{28}\text{Si}$, and ${}^{56}\text{Fe}$ with a power-law energy spectrum $J_0(E_0) = dN/dE_0$ with an exponential cut-off for rigidities $E_0/Z_\alpha \geq R_{\text{cut}}$:

$$J_0(E_0) \propto \sum_{\alpha} f_{\alpha} E_0^{-\gamma} \begin{cases} 1, & \text{if } \frac{E_0}{Z_{\alpha}} < R_{\text{cut}}, \\ e^{1 - \frac{E_0}{Z_{\alpha} R_{\text{cut}}}}, & \text{if } \frac{E_0}{Z_{\alpha}} \geq R_{\text{cut}}. \end{cases} \quad (2.1)$$

Here, $N(E_0)$ is the number of particles emitted with energy E_0 , Z_{α} is the atomic number of element $\alpha \in \{\text{H, He, N, Si, Fe}\}$, R_{cut} is the cut-off rigidity, f_{α} are the element fractions with $\sum_{\alpha} f_{\alpha} = 1$, and γ is the spectral index. We ran our simulations until more than $5 \cdot 10^6$ particles had reached the observer. Since experiments showed that UHECR mainly consist of charged nuclei [7–9], we simulated only the propagation of such nuclei and neglected, among others, photons and neutrinos.

For the EBL we applied the model of Gilmore et al. [10] (the so-called “fiducial” model) as well as the photodisintegration cross sections from the TALYS code [11, 12] with parameters adjusted as described in [13], which is the default in CRPropa 3. Moreover, we used the EGMF model proposed in [4], which describes a relatively strong EGMF, together with reflective boundary conditions. This EGMF model is based on the Dolag model [5] for the mass distribution and the Miniati model [14] for the magnetic field in the universe. To obtain good statistics, the radius of the observer was chosen as 1 Mpc and we took particles arriving with redshifts $-0.025 < z < 0.025$ into account, ensuring that no simulated particle hit the observer more than once. We carried out simulations with (model I) and without (model II) EGMF. In both cases we allowed for different values of the source parameters f_{α} , γ , and R_{cut} and applied a fit procedure similar to that described in [3] to determine the particular parameter values for which the energy spectrum and chemical composition of the simulated UHECR arriving at the observer are in the best possible agreement with the corresponding Pierre Auger Observatory data.

2.2 Fit procedure

Differently from [3], where the simulated energy spectrum is folded with a function that models detector effects and afterwards compared with the raw data from the Pierre Auger Observatory, our fit procedure for convenience fits the simulated energy spectrum to the published Pierre Auger Observatory data for the energy spectrum [15] that have been adjusted for detector effects. When fitting the energy spectrum, we took only experimental data above 5 EeV, i.e., above the so-called “ankle” of the experimental energy spectrum [15], into account, since the data for lower energies can have a considerable galactic contribution.

The Pierre Auger Observatory does not directly measure the chemical composition of the UHECR arriving at Earth, but instead observes the longitudinal profile of extensive air showers and measures the position of the maximum of energy deposition per atmospheric slant depth, commonly called “depth of the shower maximum” X_{max} [16]. Measuring the composition-sensitive quantity X_{max} is currently the most reliable technique to achieve information about the mass composition of UHECR. Therefore, we translated our simulation results for the chemical composition of the arriving UHECR into a distribution of the quantity X_{max} to allow for a direct comparison with the experimental data. For this purpose, we used the common parametrization of the X_{max} distribution for particles arriving with energy E and mass number A by generalized Gumbel functions [17], which are based on air-shower simulations with the CONEX code [18] and the EPOS-LHC model

for hadronic interactions [19]. In order to take detector effects into account, we multiplied the resulting Gumbel distribution with the energy-dependent detector acceptance and convolved this product with the energy-dependent detector resolution [16].

To determine the source properties (i.e., the values of f_α , γ , and R_{cut}) that describe the data from the Pierre Auger Observatory best, we minimized the deviance $D = D_J + D_{X_{\text{max}}}$ with $D_J = -2\ln(\mathcal{L}_J/\mathcal{L}_J^{\text{sat}})$ and $D_{X_{\text{max}}} = -2\ln(\mathcal{L}_{X_{\text{max}}}/\mathcal{L}_{X_{\text{max}}}^{\text{sat}})$ with respect to f_α , γ , and R_{cut} . Here, \mathcal{L}_J and $\mathcal{L}_{X_{\text{max}}}$ are the likelihood values of the simulated energy spectrum and X_{max} distribution, respectively, for certain values of f_α , γ , and R_{cut} . Furthermore, $\mathcal{L}_J^{\text{sat}}$ and $\mathcal{L}_{X_{\text{max}}}^{\text{sat}}$ are the likelihood values corresponding to \mathcal{L}_J and $\mathcal{L}_{X_{\text{max}}}$ for the saturated model that perfectly describes the experimental data (see [3] for details). The minimal deviance $D_{\text{min}} = D_{\text{min}}^J + D_{\text{min}}^{X_{\text{max}}}$ with the contributions D_{min}^J and $D_{\text{min}}^{X_{\text{max}}}$ from the energy spectrum and X_{max} distribution, respectively, quantifies the goodness of fit. To estimate the uncertainties in the best-fit values of the parameters γ , and R_{cut} that originate from uncertainties in the data from the Pierre Auger Observatory, we applied the same method as has been used to obtain the uncertainties given in Tab. 8 in [3].

3. Results

When considering models I and II with and without an EGMF, respectively, and fitting the element fractions f_α with $\alpha \in \{\text{H, He, N, Si, Fe}\}$, the spectral index γ , and the cut-off rigidity R_{cut} to the Pierre Auger Observatory data by minimizing the deviance D , we obtain the best-fit parameter values and the corresponding minimal deviances shown in Tab. 1.

Model	γ	$\log_{10}(\frac{R_{\text{cut}}}{\text{eV}})$	$f_{\text{H}}/\%$	$f_{\text{He}}/\%$	$f_{\text{N}}/\%$	$f_{\text{Si}}/\%$	$f_{\text{Fe}}/\%$	$D_{\text{min}} = D_{\text{min}}^J + D_{\text{min}}^{X_{\text{max}}}$
I	$1.61^{+0.08}_{-0.07}$	$18.88^{+0.03}_{-0.07}$	3.0	2.1	73.5	21.0	0.4	$191.9 = 37.3 + 154.6$
II	$0.61^{+0.05}_{-0.06}$	$18.48^{+0.01}_{-0.02}$	11.0	13.8	67.9	7.2	0.1	$221.3 = 48.7 + 172.6$
see [3]	$0.87^{+0.08}_{-0.06}$	$18.62^{+0.02}_{-0.02}$	0	0	88	12	0	$191.9 = 29.2 + 162.7$

Table 1: Best-fit parameter values of γ , R_{cut} , and f_α with $\alpha \in \{\text{H, He, N, Si, Fe}\}$ obtained by minimizing the deviance D as well as the minimal deviance D_{min} and the contributions D_{min}^J and $D_{\text{min}}^{X_{\text{max}}}$ for our models I (with EGMF) and II (without EGMF). For comparison, the results of the 1D simulations from [3] are also shown.

Obviously, the best-fit parameter values of f_α , γ , and R_{cut} depend strongly on the chosen EGMF. The minimal deviance D_{min} in Tab. 1 is smaller for model I than for model II, showing that our model with an EGMF is in better agreement with the Pierre Auger Observatory data than our model without an EGMF. For comparison, also the results of the previous global fit to the experimental data [3], which is based on 1D simulations of the UHECR propagation using a homogeneous source distribution and considering no EGMF, are shown in Tab. 1.¹ Interestingly, when extending to the 4D simulations with discrete sources following the local mass distribution of the universe and without EGMF (model II), γ and R_{cut} remain similar, whereas the deviance increases. In contrast, when including the EGMF in the 4D simulations (model I), γ and R_{cut} strongly increase and the deviance is found to be at the same level as for the 1D simulations. This shows that the EGMF has a stronger effect on the simulation results than the source distribution. In particular,

¹The fit procedure used in [3] is slightly different from the one used in the current work, but we expect that this has only a negligible effect on the results.

neglecting the EGMF leads to hard spectral indices ($\gamma < 1$), whereas including the EGMF leads to softer spectral indices ($\gamma > 1$). This is an important finding, since most UHECR acceleration models predict $\gamma > 1$. Following [20] this result could be interpreted as an effect of magnetic horizons and magnetic suppression. Furthermore, all models in Tab. 1 show a high nitrogen fraction f_N and a low iron fraction f_{Fe} , suggesting that the chemical composition of the UHECR at their sources is nitrogen-dominated.

If we use our best-fit parameter values from Tab. 1 and simulate the propagation of UHECR from their sources to Earth, we obtain results that can directly be compared to the Pierre Auger Observatory data. Figure 1 shows the simulated energy spectrum and the first and second moments of the simulated X_{\max} distribution for the best-fit parameter values of model I as well as the corresponding data from the Pierre Auger Observatory. It is apparent that these simulation results and the Pierre Auger Observatory data are in good agreement. Note that in Fig. 1(a) the additional curves show the contributions to the energy spectrum that stem from observed nuclei of different mass numbers A .

Besides the global minimum of the deviance D , which is strongly pronounced, there is only one distinct local (second) minimum of D at $\gamma \approx 2$, which was previously reported in [3] and thus seems to be a common feature independent of the particular model. The agreement of the simulation results and experimental data is less good when the parameter values of f_α , γ , and R_{cut} for the local (second) minimum of D are used. Table 2 shows these values together with the corresponding values of the deviance D , which are larger than in Tab. 1. The simulation results corresponding to the second minimum of D are still in good agreement with the Pierre Auger Observatory data for the energy spectrum (see the values of D_J), but the agreement is worsened when comparing the results for the X_{\max} distribution (see the values of $D_{X_{\max}}$).

Model	γ	$\log_{10}(\frac{R_{\text{cut}}}{\text{eV}})$	$f_H/\%$	$f_{He}/\%$	$f_N/\%$	$f_{Si}/\%$	$f_{Fe}/\%$	$D = D_J + D_{X_{\max}}$
I	$2.30^{+0.02}_{-0.02}$	$20.00^{+0.14}_{-0.08}$	12.7	5.2	38.3	42.5	1.3	$243.0 = 45.8 + 197.2$
II	$2.01^{+0.03}_{-0.03}$	$19.90^{+0.10}_{-0.09}$	1.0	35.5	17.2	44.9	1.4	$286.9 = 24.2 + 262.7$

Table 2: The same as in Tab. 1, but now for the local (second) minimum instead of the global minimum of the deviance D corresponding to our models I and II.

When investigating the effect of the evolution of the sources, the EGMF was usually neglected in the past (see, e.g., [21]). To close this gap, we parameterized similar as in [3] the emissivity of the sources with $\propto (1+z)^m$, where z is the redshift of the sources and m is a source evolution parameter. The results for the best-fit parameter values of γ and R_{cut} of model I for different source evolutions are shown in Tab. 3. From the considered source evolution parameters the value $m = 3$ shows the best agreement with the experimental data. When m becomes smaller, the agreement decreases and the spectral index γ increases. Assuming a negative source evolution with $m \approx -6$ results in compatibility of the data with first-order Fermi acceleration of UHECR or other acceleration mechanisms leading to emission spectra with a spectral index of about 2. When neglecting the EGMF, even more negative source evolutions would be required for compatibility of the data with first-order Fermi acceleration [3, 21].

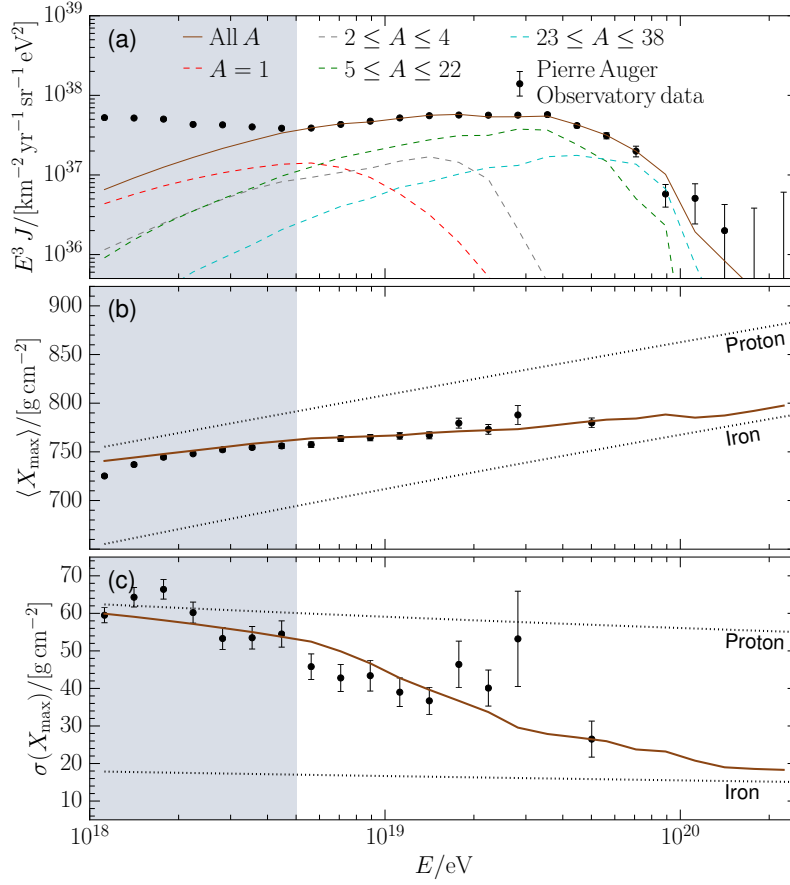


Figure 1: (a) Energy spectrum $J(E)$ [15] as well as (b) mean $\langle X_{\max} \rangle$ and (c) standard deviation $\sigma(X_{\max})$ of the X_{\max} distribution [16] for the Pierre Auger Observatory data (data points with error bars) and for our simulation results (brown solid curves). The simulation results shown here correspond to the best-fit parameter values of f_α , γ , and R_{cut} for model I (see Tab. 1) and are in good agreement with the experimental data. In (a) the additional curves show the contributions to the energy spectrum that stem from detected nuclei of different mass numbers A . The black dotted lines in (b) and (c) indicate the simulation results that one would obtain if the sources were emitting only protons (upper lines) or iron nuclei (lower lines). The Pierre Auger Observatory data with energies below the “ankle” at ≈ 5 EeV (gray regions) were not taken into account in the fit procedure described in Sec. 2.2, since they can have a considerable galactic contribution.

4. Conclusions

Based on elaborate 4D simulations of the propagation of UHECR we have studied i) for which energy spectrum and chemical composition of the UHECR at their sources the simulated energy spectrum and chemical composition at Earth are in the best possible agreement with the latest data from the Pierre Auger Observatory and ii) how the source parameters describing the reconstructed initial energy spectrum and chemical composition are affected by the EGMF. Our simulations take account of all three spatial degrees of freedom, the cosmological time-evolution of the universe, a discrete source distribution that follows the local mass distribution of the universe, and a structured EGMF.

m	γ	$\log_{10}(\frac{R_{\text{cut}}}{\text{eV}})$	$f_{\text{H}}/\%$	$f_{\text{He}}/\%$	$f_{\text{N}}/\%$	$f_{\text{Si}}/\%$	$f_{\text{Fe}}/\%$	$D_{\text{min}} = D_{\text{min}}^J + D_{\text{min}}^{X_{\text{max}}}$
3	$1.20^{+0.06}_{-0.07}$	$18.70^{+0.02}_{-0.02}$	2.3	4.0	78.4	15.0	0.3	$184.0 = 28.2 + 155.8$
0	$1.61^{+0.08}_{-0.07}$	$18.88^{+0.03}_{-0.07}$	3.0	2.1	73.5	21.0	0.4	$191.9 = 37.3 + 154.6$
-3	$1.78^{+0.07}_{-0.08}$	$18.77^{+0.03}_{-0.05}$	27.6	5.7	50.8	15.4	0.5	$199.0 = 41.2 + 157.8$
-6	$1.95^{+0.06}_{-0.10}$	$18.77^{+0.03}_{-0.04}$	29.3	5.8	47.2	17.0	0.7	$202.0 = 40.5 + 161.5$
-9	$2.05^{+0.08}_{-0.09}$	$18.78^{+0.02}_{-0.02}$	29.0	6.5	46.3	17.4	0.8	$203.4 = 42.2 + 161.2$

Table 3: Best-fit parameter values of γ , R_{cut} , and f_{α} with $\alpha \in \{\text{H}, \text{He}, \text{N}, \text{Si}, \text{Fe}\}$ obtained by minimizing the deviance D as well as the minimal deviance D_{min} and the contributions D_{min}^J and $D_{\text{min}}^{X_{\text{max}}}$ for model I and different values of the source evolution parameter m .

The results of our simulations show that the source parameters reconstructed from the Pierre Auger Observatory data depend strongly on the EGMF. Assuming an EGMF leads to soft spectral indices (> 1), whereas neglecting the EGMF leads to harder spectral indices. This behavior is qualitatively consistent with predictions of [20]. Moreover, for both situations the Pierre Auger Observatory data suggest that the chemical composition of the UHECR at their sources is dominated by intermediate-mass nuclei, which is in accordance with previous 1D simulations [3]. The source parameters deduced from the local (second) minimum of the deviance are well in line with a spectral index of about 2, but are disfavored, since they miss to reproduce the change of the mass composition observed in the Pierre Auger Observatory data.

We also found that the assumed source evolution affects the reconstructed source parameters. In the presence of an EGMF a positive source evolution parameter shows the best agreement with the experimental data. For decreasing values of the source evolution parameter the agreement becomes worse while the spectral index becomes larger. In case of a negative source evolution parameter of ≈ -6 the spectral index is ≈ 2 and thus similar to what is predicted for first-order Fermi acceleration of UHECR. In the absence of an EGMF, even more negative source evolutions would be required to see compatibility of the data with first-order Fermi acceleration [3, 21].

For the future, it would be interesting to extend our work by comparing not only the energy spectrum and chemical composition of the simulated UHECR arriving at Earth but also the anisotropy in their arrival directions with the corresponding data collected by the Pierre Auger Observatory [22, 23].

References

- [1] G. Sigl, *Science* **291**, 73-79 (2001)
- [2] K. Kotera and A. V. Olinto, *Annual Review of Astronomy and Astrophysics* **49**, 119-153 (2011)
- [3] A. Aab et al. (Pierre Auger Collaboration), *Journal of Cosmology and Astroparticle Physics* **2017**, 038 (2017)
- [4] R. Alves Batista et al., *Journal of Cosmology and Astroparticle Physics* **2016**, 038 (2016)
- [5] K. Dolag, D. Grasso, V. Springel and I. Tkachev, *Journal of Cosmology and Astroparticle Physics* **1**, 9 (2005)
- [6] P. Abreu et al. (Pierre Auger Collaboration), *Journal of Cosmology and Astroparticle Physics* **2013**, 009 (2013)

- [7] J. Abraham et al. (Pierre Auger Collaboration), *Astroparticle Physics* **31**, 399-406 (2009)
- [8] P. Abreu et al. (Pierre Auger Collaboration), *Advances in High Energy Physics* **2013**, 18 (2013)
- [9] R. Aloisio, D. Boncioli, A. di Matteo, A. F. Grillo, S. Petrer and F. Salamida, *Journal of Cosmology and Astroparticle Physics* **2015**, 006 (2015)
- [10] R. C. Gilmore, R. S. Somerville, J. R. Primack and A. Domínguez, *Monthly Notices of the Royal Astronomical Society* **422**, 3189-3207 (2012)
- [11] A. J. Koning, S. Hilaire and M. C. Duijvestijn, in *AIP Conference Proceedings*, vol. 769, pp. 1154-1159, 2005
- [12] A. J. Koning and D. Rochman, *Nuclear Data Sheets* **113**, 2841-2934 (2012)
- [13] R. Alves Batista, D. Boncioli, A. di Matteo, A. van Vliet and D. Walz, *Journal of Cosmology and Astroparticle Physics* **2015**, 063 (2015)
- [14] G. Sigl, F. Miniati and T. A. Ensslin, *Physical Review D* **68**, 043002 (2003)
- [15] I. Valiño for the Pierre Auger Collaboration, in *Proceedings of the 34th International Cosmic Ray Conference (ICRC 2015)*, The Hague, The Netherlands, Proceedings of Science, 271, 2015, [PoS\(ICRC2015\)271](#)
- [16] A. Aab et al. (Pierre Auger Collaboration), *Physical Review D* **90**, 122005 (2014)
- [17] M. De Domenico, M. Settimo, S. Riggi and E. Bertin, *Journal of Cosmology and Astroparticle Physics* **2013**, 050 (2013)
- [18] T. Pierog et al., *Nuclear Physics B-Proceedings Supplements* **151**, 159-162 (2006)
- [19] T. Pierog, I. Karpenko, J. Katzy, E. Yatsenko and K. Werner, *Physical Review C* **92**, 034906 (2015)
- [20] S. Mollerach and E. Roulet, *Journal of Cosmology and Astroparticle Physics* **2013**, 013 (2013)
- [21] A. M. Taylor, M. Ahlers and D. Hooper, *Physical Review D* **92**, 063011 (2015).
- [22] A. Aab et al. (Pierre Auger Collaboration), *Astrophysical Journal* **802**, 111 (2015)
- [23] A. Aab et al. (Pierre Auger Collaboration), *Astrophysical Journal* **804**, 15 (2015)